

Confirmation of quark-hadron duality in the neutron F_2 structure function

S. P. Malace¹, Y. Kahn^{2,3}, W. Melnitchouk³, C. E. Keppel^{3,4}

¹*University of South Carolina, Columbia, South Carolina 29208*

²*Northwestern University, Evanston, Illinois 60208*

³*Jefferson Lab, Newport News, Virginia 23606*

⁴*Hampton University, Hampton, Virginia 23668*

We apply a recently developed technique to extract for the first time the neutron F_2^n structure function from inclusive proton and deuteron data in the nucleon resonance region, and test the validity of quark-hadron duality in the neutron. We establish the accuracy of duality in the low-lying neutron resonance regions over a range of Q^2 , and compare with the corresponding results on the proton and with theoretical expectations. The confirmation of duality in both the neutron and proton opens the possibility of using resonance region data to constrain parton distributions at large x .

The quest to understand the strong interactions at intermediate energies, and particularly the transition from quark-gluon to hadron degrees of freedom, is one of the main outstanding challenges in modern nuclear physics. Considerable attention has been focused recently on the “duality” between quark and hadron descriptions of observables in electron-hadron scattering. A classic example is the finding [1] that inclusive structure functions in the region dominated by the nucleon resonances on average resemble the structure functions measured in the deep inelastic scattering (DIS) region at higher energies.

With the availability of high-precision data from Jefferson Lab and elsewhere, duality has now been firmly established for the proton F_2 and F_L structure functions [2–4], and exploratory studies in spin-dependent and semi-inclusive scattering have provided tantalizing glimpses of the flavor and spin dependence of duality (for a review see Ref. [5]). A complete picture of the workings of duality in the nucleon can only be constructed, however, with information on duality in the *neutron*, on which little empirical data exists.

Calculations based on quark models point to intriguing differences between duality in the proton and neutron [6], and some arguments even suggest that duality in the proton may be due to accidental cancellations between quark charges, which do not occur for the neutron [7]. Confirmation of duality in the neutron would therefore firmly establish that the phenomenon is not accidental, but rather a robust feature of nucleon structure functions. More generally, understanding the transition between the resonance and DIS regions can lead to better constraints on parton distribution functions (PDFs) at large momentum fractions x , by allowing data at lower final state hadron masses W to be used in global PDF fits [8, 9]. Precise knowledge of large- x PDFs, which are currently poorly constrained, is vital in searches for new physics beyond the Standard Model [10], for instance, as well as in neutrino oscillation experiments [11].

In this Letter we use a recently introduced technique [12] to extract for the first time the neutron F_2^n structure function from proton (p) and deuteron (d) F_2 data in the resonance region over a range of photon virtualities from $Q^2 = 0.6$ to 6.4 GeV². The new method is based on

an iterative approach in which the nuclear corrections are applied additively, and has been found to accurately reproduce neutron structure functions of almost arbitrary shape in both the DIS and resonance regions [12].

The extraction of reliable neutron information from deuterium data requires a careful treatment of nuclear effects [13], and we use the latest theoretical developments which allow the deuteron structure function to be analyzed in both the resonance and DIS regions, at both low and high Q^2 . In the weak binding approximation the deuteron F_2^d structure function can be written as a sum of smeared proton and neutron structure functions \tilde{F}_2^N ($N = p, n$), and an additive term which accounts for possible modification of the structure functions off-shell [12, 14, 15],

$$F_2^d = \tilde{F}_2^p + \tilde{F}_2^n + \delta^{(\text{off})} F_2^d. \quad (1)$$

The smeared nucleon structure functions are given by convolutions of the nucleon light-cone momentum distribution in the deuteron, $f_{N/d}$, and the bound nucleon structure functions [12, 14],

$$\tilde{F}_2^N = f_{N/d} \otimes F_2^N, \quad (2)$$

where the symbol \otimes denotes a convolution. The nucleon momentum distribution (or smearing) function $f_{N/d}$ accounts for the effects of the nucleon’s Fermi motion and binding, including finite- Q^2 corrections [12, 14], and is taken to be identical for the proton and neutron. The off-shell correction $\delta^{(\text{off})} F_2^d$ has been found in several models [14–16] to be typically of the order 1–2% for $x \lesssim 0.9$.

To account for the quasi-elastic (QE) tail in the deuteron data the elastic nucleon contribution is smeared using the same $f_{N/d}$. Subtracting from the deuteron F_2^d the QE contribution, together with the off-shell correction and the smeared proton \tilde{F}_2^p , one obtains an effective smeared neutron structure function \tilde{F}_2^n and then solves Eq. (2) for the neutron.

The nuclear effects are parametrized by an additive correction [12],

$$\tilde{F}_2^n = \mathcal{N} F_2^n + \delta f \otimes F_2^n, \quad (3)$$

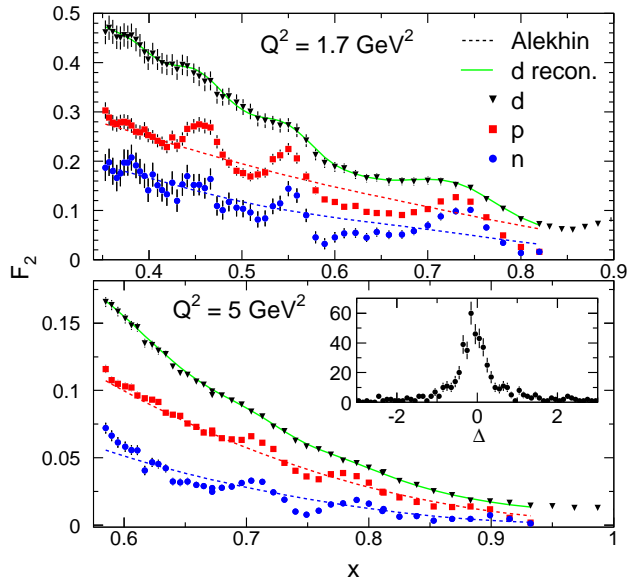


FIG. 1: Extracted neutron F_2^n structure function at $Q^2 = 1.7$ and 5 GeV^2 , together with proton and deuteron data, and the reconstructed deuteron (total uncertainties are systematic and statistical errors added in quadrature). The proton and neutron data are compared with the global QCD fit from Alekhin *et al.* [8]. The dependence of the iteration on the initial value is illustrated in the insert (see text).

where δf gives the finite width of the smearing function and \mathcal{N} its normalization. The F_2^n structure function is then extracted using an iterative procedure [12], which after one iteration gives

$$F_2^{n(1)} = F_2^{n(0)} + \frac{1}{\mathcal{N}} \left(\tilde{F}_2^n - f \otimes F_2^{n(0)} \right), \quad (4)$$

starting from a first estimate $F_2^{n(0)}$, and iterated until convergence is reached. The robustness of this method and its ability to reliably estimate errors on the extracted neutron function were investigated extensively for smooth functions in Ref. [12]. Since the smearing function is sharply peaked, the convergence of this method is typically extremely fast, requiring only one or two iterations before the F_2^d function reconstructed from the extracted F_2^n matches the original data to within experimental uncertainties.

In this analysis we use proton and deuteron F_2 data from JLab experiment E00-116 [4] and SLAC experiments E49a6 and E49a10 [17]. The former span the high- Q^2 region, $4.5 \leq Q^2 \leq 6.4 \text{ GeV}^2$, while the latter cover the lower Q^2 range, $0.6 \leq Q^2 \leq 2.4 \text{ GeV}^2$, providing a total of 514 data points. Because the extraction method requires proton and deuteron F_2 data at fixed Q^2 , the centering of the data at the same Q^2 was made at the cross section level using the p and d fits from Ref. [18]. To test the sensitivity of the results to the choice of the bin-centering fit, an additional fit was used for each target

[4, 19, 20] and half the difference in the results assigned as a systematic uncertainty.

The stability of the iteration method relies on the availability of relatively smooth data, especially for deuterium (irregularities in proton data are smoothed out by the smearing). This is critical at large x where the structure functions are small, and discontinuities could even render the extracted neutron results negative. It is particularly important that the QE contribution to the deuteron F_2^d be accounted for in the analysis, and we model this using the same smearing function, $f_{N/d}$, and nucleon form factors from Refs. [21, 22]. This is found to provide a good description of the QE peak as a function of Q^2 .

An example of the extracted neutron F_2^n structure function is displayed in Fig. 1 for $Q^2 = 1.7$ and 5 GeV^2 , together with the input proton and deuteron data (the complete data set will be shown in Ref. [23]). The starting value of the neutron for the iteration was $F_2^{n(0)} = F_2^p$, and the deuteron F_2^d reconstructed from the proton and extracted neutron was found to be in good agreement with the data after two iterations. The spectrum of the F_2^n structure function in the resonance region displays similar characteristics as observed from the proton spectrum: one finds three resonant enhancements which fall with Q^2 at a similar rate as for the proton.

To check that the extracted neutron structure function does not depend on the starting value of the iteration, the extraction procedure was repeated assuming a different boundary condition, $F_2^{n(0)} = F_2^p/2$. The difference between the two results $\Delta = [F_2^n(F_2^{n(0)} = F_2^p) - F_2^n(F_2^{n(0)} = F_2^p/2)]/\sigma(F_2^n)$, normalized by the total F_2^n uncertainty $\sigma(F_2^n)$, is shown in the insert of Fig. 1 after two iterations. One finds an almost Gaussian distribution centered around 0 (the mean of the distribution is around -0.07) with a width well within the typical total uncertainty of F_2^n . In fact only 6% of the total number of data points lie outside of a 2σ range. More extreme boundary conditions, such as $F_2^{n(0)} = 0$, do not alter the characteristics of the extracted F_2^n structure function spectrum, with the resonant structures already visible after just 1 iteration. On the other hand, as discussed in Ref. [12], more iterations are needed for poor choices of initial values, which increases the scatter of data points if the deuterium data in particular display any nonuniformities.

The effect of the off-shell correction $\delta^{(\text{off})} F_2^d$ was taken into account using the model of Ref. [16], which gives $\approx -1.5\%$ correction over most of the x range considered, and was argued to provide an upper limit on the correction. The F_2^d data are corrected by subtracting half of the off-shell correction from [16] and assigning a 100% uncertainty. When propagated into the F_2^n uncertainty this was found to contribute less than 2% to the total error.

In Fig. 1 we also show F_2^p and F_2^n from global QCD fits to DIS data (with $W^2 > 4 \text{ GeV}^2$) from Alekhin *et al.* [8], which illustrates the striking similarity between the QCD fit and the resonance data, reminiscent of Bloom-

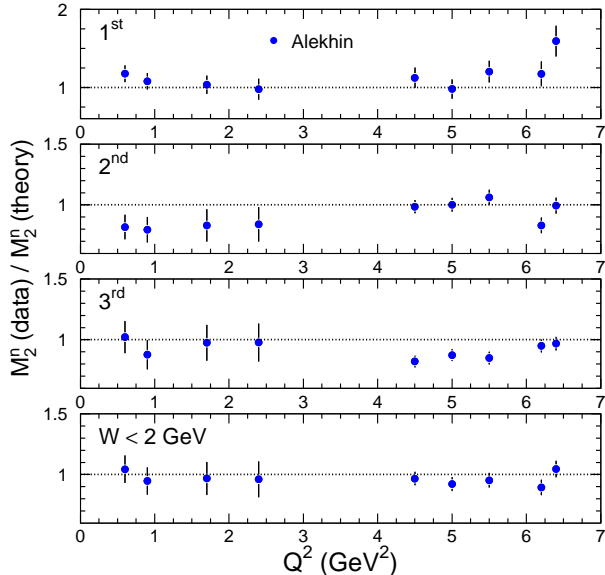


FIG. 2: Truncated neutron moments M_2^n (“data”) in various resonance regions (1st, 2nd, 3rd and $W < 2$ GeV) relative to the QCD fit from Alekhin *et al.* [8] (“theory”).

Gilman duality [1]. To quantify this duality we consider ratios of “truncated” moments M_2 [24],

$$M_2(Q^2, \Delta x) = \int_{\Delta x} dx F_2(x, Q^2), \quad (5)$$

in the resonance region for specific intervals Δx . Following previous proton data analyses [2, 4], we consider the regions

- 1st resonance region $\rightarrow W^2 \in [1.3, 1.9]$ GeV²
- 2nd resonance region $\rightarrow W^2 \in [1.9, 2.5]$ GeV²
- 3rd resonance region $\rightarrow W^2 \in [2.5, 3.1]$ GeV²

as well as the entire resonance region $1.3 \leq W^2 \leq 4$ GeV². At a given Q^2 , the lowest- W (Δ resonance) region corresponds to the highest- x range, and for a fixed W interval the larger the Q^2 , the higher the x .

The ratio of the truncated moments of the resonance data to the global QCD fit [8], computed over the same x range, is shown in Fig. 2 as a function of Q^2 . Globally, the agreement between the QCD fit and the resonance data is quite remarkable, with deviations of $\lesssim 10\%$ observed over the entire Q^2 range. Locally, in the individual resonance regions the deviations are generally $\lesssim 15 - 20\%$, somewhat larger only in the 1st resonance region at the largest Q^2 . This is not surprising given the fact that the Δ region at $Q^2 = 6.4$ GeV² covers the highest- x regime studied, $x \sim 0.9$, where the QCD fit is mostly beyond its limit of applicability.

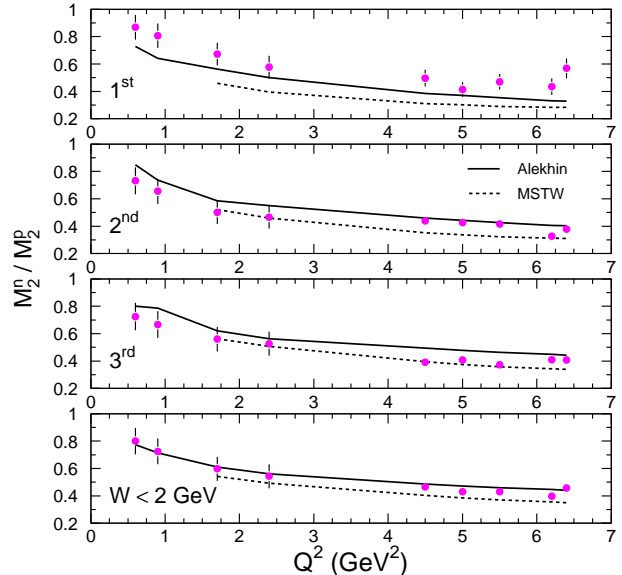


FIG. 3: Ratio of truncated neutron to proton moments M_2^n/M_2^p in various resonance regions as a function of Q^2 , compared with global QCD fits from Alekhin *et al.* [8] and MSTW [25].

The isospin dependence of duality can be studied by comparing the truncated neutron moments with the analogous proton moments. The ratio of these is displayed in Fig. 3 as a function of Q^2 for the various resonance regions, and compared with global QCD fits from Alekhin *et al.* [8] and from MSTW [25], corrected for target mass effects [26]. The MSTW fits are shown for $Q^2 \gtrsim 2$ GeV², which corresponds to their approximate limit of validity.

The ratios show good agreement with the data, with the exception of the Δ region which is somewhat underestimated. Since the proton and neutron transitions to the Δ are isovector, the resonant contributions should be identical; on the other hand, the DIS structure functions in the Δ region are expected to be rather different, with $F_2^n \ll F_2^p$, so that violation of duality here is expected to be strongest. In addition, the QCD fits are least constrained in this region due to the scarcity of large- x DIS data. This is especially the case for the MSTW fit [25] which limits the data sets to $W^2 > 15$ GeV².

The M_2^n/M_2^p ratios at fixed Q^2 are shown in Fig. 4 as a function of x for the three resonance regions, compared with the QCD fits as in Fig. 3. The global fits offer a good description of the 2nd and 3rd resonance region data, revealing clear evidence of duality down to Q^2 as low as 0.6 GeV². The fits underestimate the Δ -region ratios and this trend becomes more pronounced as one moves to larger Q^2 ($\gtrsim 4$ GeV²) and larger x . The Alekhin *et al.* fit [8] offers a better description at large x , which is likely due to its inclusion of lower- W , lower- Q^2 data.

Our results can be compared with quark model ex-

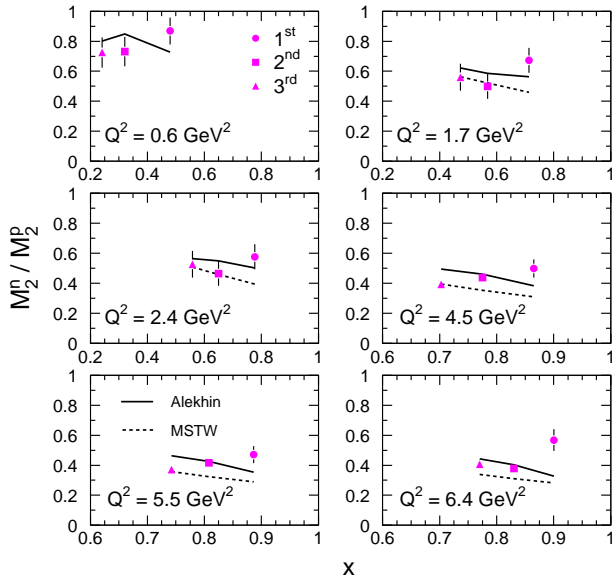


FIG. 4: As in Fig. 3 but as a function of x for fixed Q^2 .

pectations for the isospin dependence of duality, which predict systematic deviations of resonance data from local duality. Assuming dominance of magnetic coupling, the proton data are expected to overestimate the DIS function in the 2nd and 3rd resonance regions due to the relative strengths of couplings to odd-parity resonances, especially those in the quark spin- $\frac{1}{2}$ octet [6]. The neutron data are predicted to lie below the DIS curve in the 2nd resonance region due to the small coupling to octet states with spin $\frac{1}{2}$, but have larger couplings to odd-parity quark spin- $\frac{3}{2}$ octet states. Remarkably, the neutron data do indeed underestimate the global F_2^n fits

in the 2nd resonance region, just as the proton data were found to exceed the global F_2^p fits [2, 4]. Moreover, the similarity between the truncated M_2^n moments in the $W^2 < 4$ GeV² and DIS regions strongly suggests that the resonance cancellations in the proton are not accidental [7], but rather form a systematic pattern which dramatically reveals itself through the Bloom-Gilman duality phenomenon.

In conclusion, we have extracted the neutron structure function F_2^n for the first time in the resonance region from inclusive proton and deuteron data. Our comparisons of empirical truncated moments to those extracted from global QCD fits to high- W^2 data show clear signatures of Bloom-Gilman duality, with better than 15–20% agreement in the 2nd and 3rd resonance regions, and less than 10% deviations when integrated over the entire $W^2 < 4$ GeV² region. The confirmation of duality in the neutron establishes that the phenomenon is not accidental, but is a general property of nucleon structure functions. Our findings suggest that averaged resonance data could in future be used to constrain the large- x behavior of global QCD fits [8, 9] by relaxing the W^2 cuts on data down to the 2nd resonance region, $W^2 \sim 1.9$ GeV². This could also have significant impact for searches for new physics beyond the Standard Model at colliders and neutrino oscillations experiments.

Acknowledgments

We thank S. Alekhin, S. Kulagin and G. Watt for helpful communications. This work was supported by the DOE contract No. DE-AC05-06OR23177, under which Jefferson Science Associates, LLC operates Jefferson Lab, and by NSF grant PHY-0856010.

-
- [1] E. D. Bloom and F. J. Gilman, Phys. Rev. Lett. **25**, 1140 (1970).
 - [2] I. Niculescu *et al.*, Phys. Rev. Lett. **85**, 1182, 1186 (2000).
 - [3] Y. Liang *et al.*, arXiv:nucl-ex/0410027.
 - [4] S. P. Malace *et al.*, Phys. Rev. C **80**, 035207 (2009).
 - [5] W. Melnitchouk, R. Ent and C. Keppel, Phys. Rept. **406**, 127 (2005).
 - [6] F. E. Close and N. Isgur, Phys. Lett. B **509**, 81 (2001); F. E. Close and W. Melnitchouk, Phys. Rev. C **68**, 035210 (2003).
 - [7] S. J. Brodsky, arXiv:hep-ph/0006310.
 - [8] S. Alekhin *et al.*, arXiv:0908.2766 [hep-ph].
 - [9] A. Accardi *et al.*, arXiv:0911.2254 [hep-ph].
 - [10] S. Kuhlmann *et al.*, Phys. Lett. B **476**, 291 (2000).
 - [11] M. G. Albrow *et al.*, arXiv:hep-ex/0509019.
 - [12] Y. Kahn, W. Melnitchouk and S. Kulagin, Phys. Rev. C **79**, 035205 (2009).
 - [13] W. Melnitchouk and A. W. Thomas, Phys. Lett. B **377**, 11 (1996).
 - [14] S. Kulagin and R. Petti, Nucl. Phys. A **765**, 126 (2006).
 - [15] S. Alekhin, S. Kulagin and S. Liuti, Phys. Rev. D **69**, 114009 (2004).
 - [16] W. Melnitchouk, A. W. Schreiber and A. W. Thomas, Phys. Lett. B **335**, 11 (1994).
 - [17] J. S. Poucher *et al.*, Phys. Rev. Lett. **32**, 118 (1974); J. S. Poucher, Ph. D. thesis, MIT (1971).
 - [18] M. E. Christy and P. E. Bosted, arXiv:0712.3731 [hep-ph]; P. E. Bosted and M. E. Christy, Phys. Rev. C **77**, 065206 (2008).
 - [19] C. E. Keppel, Ph. D. thesis, American University (1994).
 - [20] J. Gomez *et al.*, Phys. Rev. D **49**, 4348 (1994).
 - [21] J. Arrington *et al.*, Phys. Rev. C **76**, 035205 (2007).
 - [22] P. E. Bosted, Phys. Rev. C **51**, 409 (1995).
 - [23] S. P. Malace *et al.*, in preparation.
 - [24] A. Psaker *et al.*, Phys. Rev. C **78**, 025206 (2008).
 - [25] A. D. Martin, W. J. Stirling, R. S. Thorne and G. Watt, Eur. Phys. J. C **64**, 653 (2009).
 - [26] I. Schienbein *et al.*, J. Phys. G **35**, 053101 (2008)